

Study of $^{12}\text{C}(p,p'\gamma)^{12}\text{C}$ reaction

M. Dhibar,¹ I. Mazumdar,^{2,*} G. Anil Kumar,¹ S. P. Weppner,³ A. K. Rhine Kumar,² S. M. Patel,² and P. B. Chavan²

¹*Department of Physics, Indian Institute of Technology - Roorkee, 247667, INDIA*

²*Department of Nuclear and Atomic Physics, Tata Institute of Fundamental Research, Mumbai - 400005, INDIA*

³*Eckerd College, St. Petersburg, FL. 33711, USA*

(Dated: June 7, 2018)

In the present work, we report our in depth study of $^{12}\text{C}(p,p'\gamma)^{12}\text{C}$ reaction both experimentally and theoretically with proton beam energy ranging from 8 MeV to 22 MeV. The angular distributions were measured at six different angles. We discuss the gamma angular distributions, total cross sections values for 4.438, 9.64, 12.7 and 15.1 MeV states. We also describe the theoretical interpretation of our measurements using optical model analysis. We also report the branching ratios from our measurements. For the first time, we have measured the the cross section and branching ratio for the 9.64 MeV state.

I. INTRODUCTION

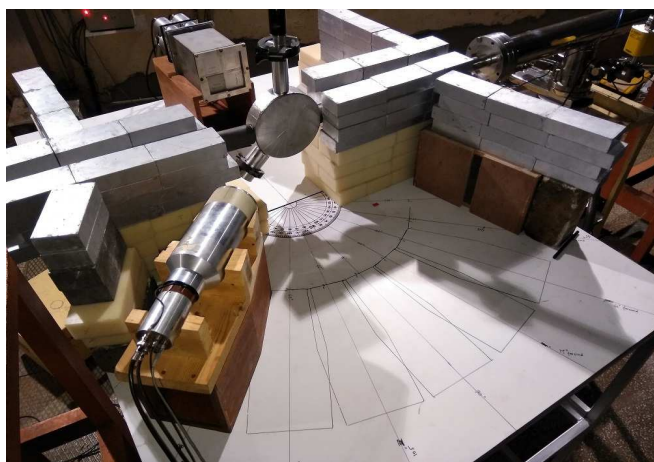


FIG. 1. Experimental arrangement used during $^{12}\text{C}(p,p'\gamma)^{12}\text{C}$ measurements.

Study of the $^{12}\text{C}(p,p'\gamma)^{12}\text{C}$ inelastic scattering reaction touches on important topics in nuclear reactions and structural studies. Understanding this reaction in terms of scattering theory involves two steps: first, the excitation, then by the de-excitation of the ^{12}C nucleus. These steps are not equally understood. Deexcitation process is relatively simpler to understand. It is the release of energy via a gamma ray with a known energy and angular momentum. However, understanding the excitation mechanism raises a variety of questions. Is the state under consideration excited into a collective mode or is it better understood by a single nucleon excitation, or do both representations have validity? How important is the exchange process for identical particles? The role of alpha particle clustering in ^{12}C nucleus is also to be understood? The influence of giant resonance states in ^{12}C and energy levels of ^{13}N may be important in the analy-

sis. All of these interesting questions motivate us experimentally and theoretically to study the $^{12}\text{C}(p,p'\gamma)^{12}\text{C}$ reaction with proton beam energy from 8 MeV to 22 MeV. As of today, no optical model theory exists which can successfully explain excited states (namely, 4.43 MeV, 9.64 MeV, 12.71 MeV and 15.1 MeV) of ^{12}C for this beam energy range. The lowest projectile energy that has been discussed in the literature is 40 MeV [1]. There were few attempts to formulate a microscopic proton-nucleus theory below this energy range, specifically by Jeukenne, Lejeune and Mahaux [2] and Brieva Rook[3]. These theories were applied only to $^{12}\text{C}(p, p)$ (only the elastic channel) at energies used in the present work (14 MeV - 40 MeV). However, several authors [4, 5] have struggled to fit the elastic data with their microscopic theories. Therefore, the scattering of proton in the energy range of 8 to 30 MeV poses challenge to theorists even though the optical model [6] formalism works well at higher energies.

Experimentally, there exist very few data for the cross section measurement of 12.71 MeV and 15.1 MeV states [7–10]. There exist no data on the cross sections for 9.64 MeV state. However, many studies on 4.43 MeV state provide cross section data [7, 11–23]. So, there is enough justification for the measurement of scattering cross sections of $^{12}\text{C}(p,p'\gamma)^{12}\text{C}$ reaction up to about 30 MeV.

The reaction also has a large significance in the astrophysical context. The occurrence of gamma-ray lines at 4.43 MeV and 15.1 MeV from solar flares carries the details of the interaction mechanism through which charged particles (namely, protons and ions) are accelerated and interact with solar flares [12, 14, 24]. Since these gamma lines are uninfluenced by solar magnetic fields, they carry the precise information about the features of the accelerated-particle population and also the identity of the accreted particles [25]. These gamma lines also provide the information about fundamental properties and conditions, such as, abundance of the elements, temperature and density of the solar flares ambience and accelerated ion-parameters. The flux ratio of $f_{15.1}/f_{4.43}$ from $^{12}\text{C}(p,p'\gamma)^{12}\text{C}$ produced during solar flares can give the information about cross section as well as the relative isotropic abundance ratio of ^{12}C and ^{16}O [26, 27].

* indra@tifr.res.in

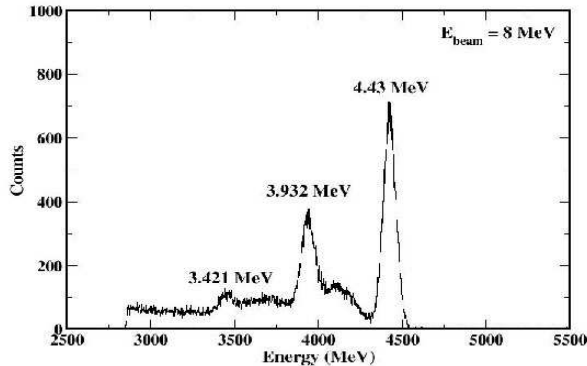


FIG. 2. A typical 4.438 MeV gamma spectrum from $^{12}\text{C}(p,p'\gamma)^{12}\text{C}$ reaction at $E_p = 8$ MeV.

In the present work, we have measured the differential and total gamma cross sections and gamma branching ratios to the ground state for all the states studied. The paper is categorized in following sections. The experimental details are given in Section-2. In Section-3 we have described the measurements and data analysis. Section-4 discusses the GEANT4 simulations and the efficiency calculation of the detector. Details of theoretical formalism i.e optical model analysis are discussed in Section-5. In Section-6, we provide the results of measurements along with a detailed theoretical analysis. Section-7 presents the summary.

II. EXPERIMENTAL DETAILS

The $^{12}\text{C}(p,p'\gamma)^{12}\text{C}$ reaction was carried out by bombarding proton beam on mylar target of thickness 2.22 mg/cm^2 . The proton beam was obtained from 14 MV Pelletron at TIFR, Mumbai[28]. The experiment was performed using proton beam ranging from 8 MeV to 22 MeV. The gamma rays produced from inelastic scattering were detected using a $3.5'' \times 6''$ large volume cylindrical $\text{LaBr}_3:\text{Ce}$ detector[29]. The gamma angular distributions were measured at six different angles (60° , 75° , 90° , 105° , 120° , 135°) w.r.t to beam direction by keeping the detector at a distance 35 cm from the scattering chamber. The detector was shielded using lead bricks at all possible direction to reduce the background events produced during the experiment. The beam was stopped on a Faraday cup beyond the target and total charge was measured using a beam current integrator. The energy loss of the beam in the target was found to be less than one MeV using SRIM code [30]

The recorded energy and timing signals from the detector were further processed using standard Nuclear Instrumentation Module (NIM) electronics. The timing signal from anode was fed to the Time to Amplitude

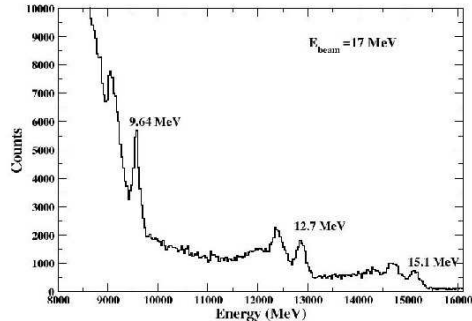


FIG. 3. A gamma spectrum showing 9.64, 12.7 and 15.1 MeV from $^{12}\text{C}(p,p'\gamma)^{12}\text{C}$ reaction measured at $E_p = 17$ MeV.

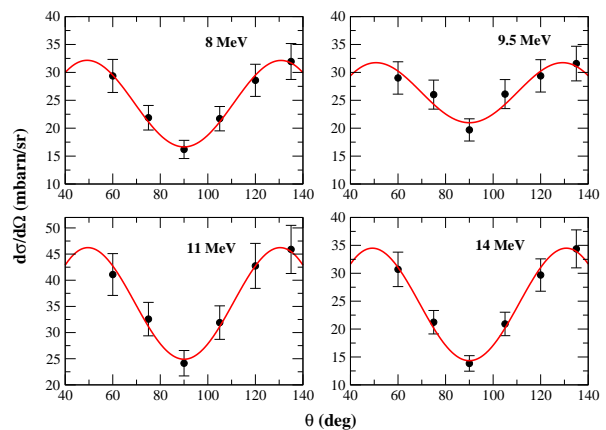


FIG. 4. Angular distribution of γ -rays obtained for 4.44 MeV state.

converter (TAC) as a start signal. Pileup rejection was achieved using the zero-cross technique[31]. The shaped and amplified energy signal was recorded in a peak sensing ADC and data were collected in events mode. Energy calibration of the detector was carried out using standard gamma sources, namely, ^{137}Cs (661.6 keV), ^{60}Co (1173, 1332 keV) and ^{22}Na (511, 1274 keV). Am-Be source was used for 4.44 MeV gamma-rays. This ensures the energy calibration and linearity check from few hundred keV to 4.433 MeV. The energy gain of the detector was checked periodically during the experiment, and was found to be stable. The 4.44 MeV gamma spectrum at $E_p = 8$ MeV is shown in Fig.2. The gamma spectrum showing three energy states of ^{12}C nucleus, namely, 9.64, 12.7, 15.1 MeV measured at $E_p = 17$ MeV is presented in Fig. 3. Clearly the use of $\text{LaBr}_3:\text{Ce}$ detector has ensured recording spectra with quality much better than those reported using a $\text{NaI}(\text{Tl})$ detector [7]. The Table-I summarises our experimental measurements.

III. MEASUREMENT AND ANALYSIS METHOD

Gamma angular distributions were measured for the energy levels of ^{12}C nucleus, namely, 4.438, 9.64, 12.71 and 15.11 MeV using inelastic scattering of protons on ^{12}C . The background subtracted γ ray yields were corrected for efficiencies of the detector for all the gamma rays to get the differential cross sections. For gamma-ray with yield Y , recorded at an angle θ , with a solid angle $d\Omega$, the differential cross section can be written as

$$Y = N_p N_t (d\Omega \epsilon) \left[\frac{d\sigma}{d\Omega}(\theta, E_p) \right] \quad (1)$$

where N_p defines the incident beam particles, N_t is the number of carbon nuclei per unit area and the absolute photopeak efficiency of the detector is ϵ which is calculated using GEANT4 simulation [32]. The gamma angular distribution of differential cross section was fitted using Legendre polynomial functions as given below

$$\frac{d\sigma}{d\Omega} = \sum_{l=0; l=even}^{l=l_{max}} a_l P_l(\cos\theta) \quad (2)$$

where the first term a_l is a free parameter obtained by fitting data with the eq. 2. The second term is the Legendre polynomial function with order l . The l_{max} should be less than two times the gamma multipolarity. The total gamma cross section can be obtained by integrating eq. 2 for the differential cross section to obtain $4\pi a_0$, where a_0 is the coefficient of the Legendre polynomial function after fitting the differential cross sections. Therefore, the total cross section can be written as,

$$\sigma_{total} = 4\pi a_0 \quad (3)$$

IV. SIMULATION

The total detection efficiency of the detector for gamma rays is the product of the intrinsic and geometric efficiencies. In order to make the simulations more realistic, we have included the detector geometry, the wooden support structure for the detector and all the absorbing materials between the target and the face of the detector. The low energy EM Physics package[33] was used in the physics list class. The radioactive decay module has been used to simulate the decay of the point sources, namely, ^{137}Cs (661.6 keV), ^{60}Co (1173, 1332 keV), ^{22}Na (511, 1274 keV), Am-Be(4.438 MeV) and 5.5 MeV γ -rays [34]. The energies and branching ratios of the γ -sources used in the simulation were taken from NNDC website[35]. The simulations were done considering an isotropic emission of γ -rays by assuming a point source. Total sample of 10^6 γ -ray events were generated and distributed over the detector surface.

V. RESULTS AND DISCUSSION

We present here the results of our measurements, namely, angular distributions, differential and total cross sections and branching ratios of the 4.43, 9.64, 12.7 and 15.1 MeV states. Theoretical interpretations of the data are also presented in this section.

A. Excitation function of 4.438 MeV level of ^{12}C nucleus

The angular distributions and the total cross sections were measured for 4.44 MeV state at beam energies ranging from 8 to 14 MeV. A typical gamma-ray spectrum showing the 4.44 MeV transition measured at 90° with respect to the beam direction is shown in Fig. 2. This spectrum corresponds to proton beam energy of 8 MeV. The clear separation of the photopeak, first- and second-escape peaks show the high resolving power of $\text{LaBr}_3(\text{Ce})$ detector. This can be contrasted with the gamma-ray spectra measured earlier with $\text{NaI}(\text{Tl})$ detectors with much inferior energy resolution as discussed in [7]. Needless to say, the present measurements are aimed towards generating many more precision data than reported earlier. Angular distributions of the gamma-rays for some of the beam energies are shown in Fig. 4. The solid lines are the best fits using Legendre polynomials. Our method of measuring the cross sections for populating a specific state from the gamma decay of the state has potential complications. Increasing the beam energy leads to population of higher lying states above the state under consideration. Their decay can feed to the lower state under consideration by gamma emission, resulting in a higher observed cross section than the direct production cross section of the state under consideration. In the present case, the production cross section of the 4.44 MeV state has been measured in the rather low energy domain of 8 to 14 MeV. For these energies the population of states higher than 4.44 MeV (namely, 7.65, 9.64 and 12.7 MeV) and their subsequent feeding to 4.44 MeV is minuscule. It should be noted that the Hoyle state at 7.65 MeV and the 9.64 MeV state predominantly decay by alpha channel. This coupled with the fact that 4.44 MeV state has 100% gamma branching ratio to the ground state tells us that the measured cross sections of 4.44 MeV state obtained from $(p, p' \gamma)$ reaction (present case) should be equal to cross sections obtained from (p, p') data. As discussed in the theory section there is a strong influence of resonances in the excitation function of 4.44 MeV state. This typical structure of the excitation function is often used to verify ^{13}N resonances in a strong coupling model [9, 18, 36]. The data (gamma) from Kiener *et al.*, [14] show a sharp rise in cross-section at 8.3 MeV, 9.1 MeV, 10.5 MeV, 11.0 MeV, 12.7 MeV, and 13.8 MeV. Many of these rises are at the threshold of higher energy states in the ^{12}C nucleus ($8.3\text{MeV} \rightarrow 7.65\text{MeV}(0^+), 10.5\text{MeV} \rightarrow$

TABLE I. Summary of the present measurements for 4.44, 9.64, 12.7 and 15.1 MeV states.

| State (MeV) | Beam Energy (MeV) | Angle (θ) |
|----------------|----------------------|---|
| 4.43 | 8 | $60^\circ, 75^\circ, 90^\circ, 105^\circ, 120^\circ, 135^\circ$ |
| | 8.5 | $60^\circ, 75^\circ, 90^\circ, 105^\circ, 120^\circ, 135^\circ$ |
| | 9 | $60^\circ, 75^\circ, 90^\circ, 105^\circ, 120^\circ, 135^\circ$ |
| | 9.5 | $60^\circ, 75^\circ, 90^\circ, 105^\circ, 120^\circ, 135^\circ$ |
| | 10 | $60^\circ, 75^\circ, 90^\circ, 105^\circ, 120^\circ, 135^\circ$ |
| | 11 | $60^\circ, 75^\circ, 90^\circ, 105^\circ, 120^\circ, 135^\circ$ |
| | 12 | $60^\circ, 75^\circ, 90^\circ, 105^\circ, 120^\circ, 135^\circ$ |
| | 13 | $60^\circ, 75^\circ, 90^\circ, 105^\circ, 120^\circ, 135^\circ$ |
| 9.64 | 14 | $60^\circ, 75^\circ, 90^\circ, 105^\circ, 120^\circ, 135^\circ$ |
| | 15 | $60^\circ, 75^\circ, 90^\circ, 105^\circ, 120^\circ, 135^\circ$ |
| | 16 | $60^\circ, 75^\circ, 90^\circ, 105^\circ, 120^\circ, 135^\circ$ |
| | 17 | $60^\circ, 75^\circ, 90^\circ, 105^\circ, 120^\circ, 135^\circ$ |
| | 18 | $60^\circ, 75^\circ, 90^\circ, 105^\circ, 120^\circ, 135^\circ$ |
| 12.71 | 15 | $60^\circ, 75^\circ, 90^\circ, 105^\circ, 120^\circ, 135^\circ$ |
| | 16 | $60^\circ, 75^\circ, 90^\circ, 105^\circ, 120^\circ, 135^\circ$ |
| | 17 | $60^\circ, 75^\circ, 90^\circ, 105^\circ, 120^\circ, 135^\circ$ |
| | 18 | $60^\circ, 75^\circ, 90^\circ, 105^\circ, 120^\circ, 135^\circ$ |
| 15.11 | 17 | $60^\circ, 75^\circ, 90^\circ, 105^\circ, 120^\circ, 135^\circ$ |
| | 18 | $60^\circ, 75^\circ, 90^\circ, 105^\circ, 120^\circ, 135^\circ$ |
| | 19.5 | $45^\circ, 60^\circ, 75^\circ, 90^\circ, 105^\circ, 120^\circ, 135^\circ$ |
| | 20 | 90° |
| | 20.5 | 90° |
| | 21 | 90° |
| | 21.5 | 90° |
| 22 | 90° | |

9.64 MeV (3^-), 12.7 MeV \rightarrow 11.8 MeV (2^-), 13.8 MeV \rightarrow 12.71 MeV (1^+). The gamma differential cross sections along with our calculations are shown in Fig. 5 for three beam energies. The solid blue line is the single particle model without adding resonances. The single particle model with resonances (blue dashed line) appears better than the calculation without resonances in terms of both shape and magnitude of the data. The resonances added in the calculation are listed in Table-III. The energies, parities, and isospin ($T = 0$) are taken from the compilation of Ajzenberg-Selove [37]. The theoretical calculation for 14 MeV appears to reproduce the data better than for other two energies. The reason for this is that it is closest to the broad 15.44 MeV 2^+ resonance and therefore has a significant amount of direct excitation. In contrast the 8 MeV calculation is affected most by the 7.65 MeV 0^+ level (the Hoyle state) which accentuates only the exchange state. Likewise the 9.8 MeV calculation is affected by the 9.65 MeV 3^- state and the 10.30 MeV 0^+ broad resonance which also participate in exchange. Both these calculations would benefit if there was a 2^+ resonance nearby to begin to replicate the sig-

TABLE II. Measured γ -branching ratios from $^{12}\text{C}(p,p'\gamma)^{12}\text{C}$.

| Energy (MeV) | 14 (MeV) | 18 (MeV) | 19.5 (MeV) |
|-----------------|---------------------|-------------------|-----------------|
| 9.64 | 0.0035 ± 0.0031 | | |
| 12.7 | | 0.020 ± 0.003 | |
| 15.1 | | | 0.79 ± 0.19 |

nature shape of an E2 transition which all our experimental data follow. In recent times there has been a search for a 2^+ state as part of the Hoyle band [38–42] and it has been tentatively found at (9.84 ± 0.06) MeV with a width of (1.01 ± 0.15) MeV. The Hoyle 2^+ contribution along with present calculations of the gamma differential cross-section is shown in Fig. 6. The total cross section for 4.44 MeV state is shown in Fig. 7. The experimental data are taken from Refs. [17–23, 36, 43–45] and our data are the blue diamonds. Adding the Hoyle state improves the total cross-section in the region of 8 to 10.5 MeV. The

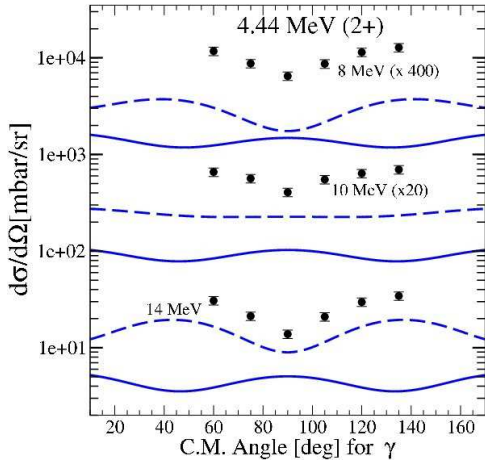


FIG. 5. The partial ($p, p'\gamma$) differential cross-section for excitation to the 4.43 MeV (2^+) energy level. The gamma data (black circle) are from the present experimental work. The blue lines are from the single particle model of this work. The solid line is the complete model without resonances added, the dashed line adds resonances listed in the Appendix A.

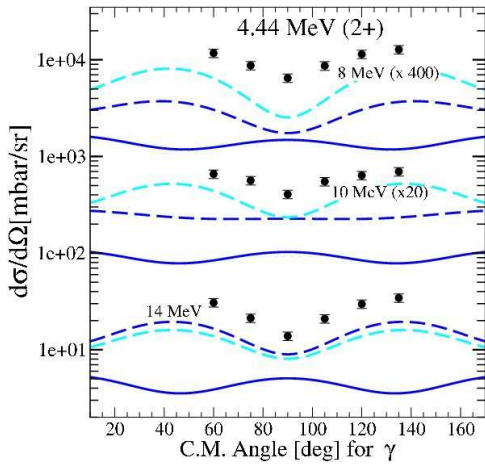


FIG. 6. The partial ($p, p'\gamma$) differential cross-section of excitation to the 4.43 MeV (2^+) energy level. The gamma data (black circle) is from the present experimental work. The blue lines are from the single particle model of this work. The solid line is the complete model without resonances added, the dashed line adds resonances listed in the Appendix A. The new light blue line has the Hoyle 2^+ state includes as a resonance at 9.85 MeV.

gamma differential cross-section is where the calculations showed a marked difference. The shape improved dramatically, thus implying a stronger E2 transition. This shows the ability of the present calculation to translate a proton excitation to a gamma de-excitation. The single particle model has its deficits, but its microscopic power gives us strong physical insight to the structural effect on the reaction mechanism at these low energies.

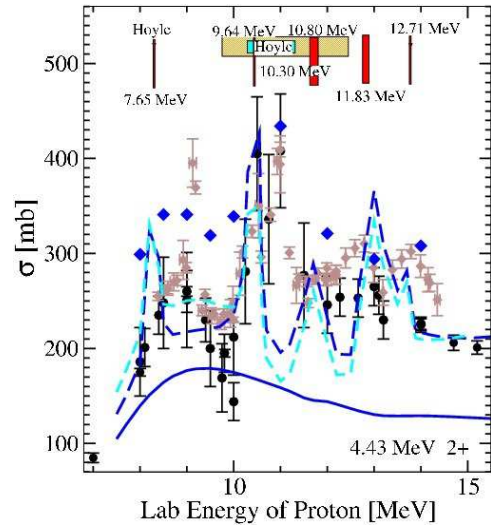


FIG. 7. The total cross-section for excitation to the 4.43 MeV (2^+) energy level. The experimental data references can be found in the text. The blue diamond data are from the present measurement. The blue lines are from the single particle model of this work. The solid line is the complete model without resonances added, the dashed line adds resonances listed in the Appendix A, the new light blue dashed line includes the Hoyle 2^+ resonance at 9.85 MeV.

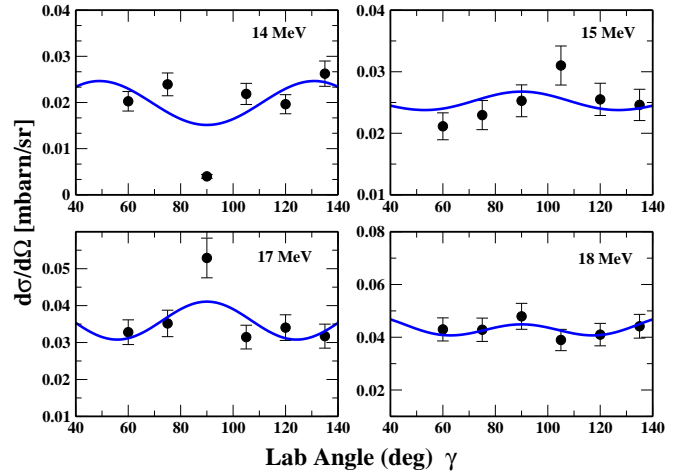


FIG. 8. Angular distribution of γ -rays obtained for 9.64 MeV state at $E_p=14, 15, 17$ and 18 MeV.

B. Excitation function of 9.64 MeV level of ^{12}C nucleus

The 9.64 MeV state is a 3^- state and also has an electric transition. The technique used for the 4.44 MeV has been used for 9.64 MeV as well. The resonances used in the calculation are discussed in the previous section. Few additional resonances are also added to improve the results (starred symbol) and are shown in the same table. These resonances are taken from Refs. [37, 46, 47]. The angular distributions were measured for four beam

energies ranging from 14 to 18 MeV and are shown in Fig. 8. The same measured differential cross-sections for four beam energies are shown again in Fig. 9 along with the theoretical calculation. For the lower beam energies (14 and 15 MeV) we obtained a good agreement in terms of shape and magnitude of the data. At the highest beam energy of 18 MeV, the difference between theory and data is significant. This is because, for the 18 MeV beam energy, there may be some feeding from the higher states to the 9.64 MeV state through gamma decay. This would enhance the measured cross section of the 9.64 MeV gamma-rays. Unlike the 4.44 MeV state which has a 100% gamma decay to the ground state, the 9.64 MeV state is a large alpha emitter. The value of the gamma branching ratio of the 9.64 MeV state has not previously been reported. In this work, we have compared our measured gamma-ray cross sections at 14 MeV beam energy with the experimental (p, p') cross section for the 9.65 MeV state reported by Harada *et al.* [44], for the same beam energy. We have found the branching fraction to be 0.0035. This value is being reported for the first time. While inclusion of resonances in our calculation is imported, it must be admitted that the addition of extra E3 strengths (Table-IV)(confusion whether to included or not??) does not lead to significant improvement in the reproduction of the data.

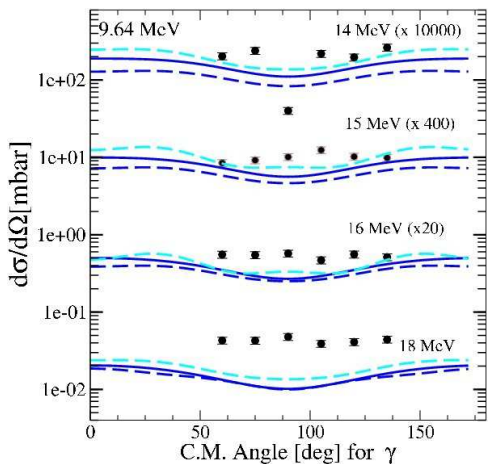


FIG. 9. The partial $(p, p'\gamma)$ differential cross-section for excitation to the 9.64 MeV (2^+) energy level. The gamma data (black circle) are from the present experimental work. The blue lines are from the single particle model of this work. The solid line is the complete model without resonances added, the dashed line adds resonances listed in the text. The new light blue line has three additional resonances of the 3^- state which are listed in the Appendix A.

C. Excitation function of 12.7 and 15.1 MeV level of ^{12}C nucleus

The 12.71 and 15.11 MeV states are the two lowest lying 1^+ states with unnatural parity of ($M1$)

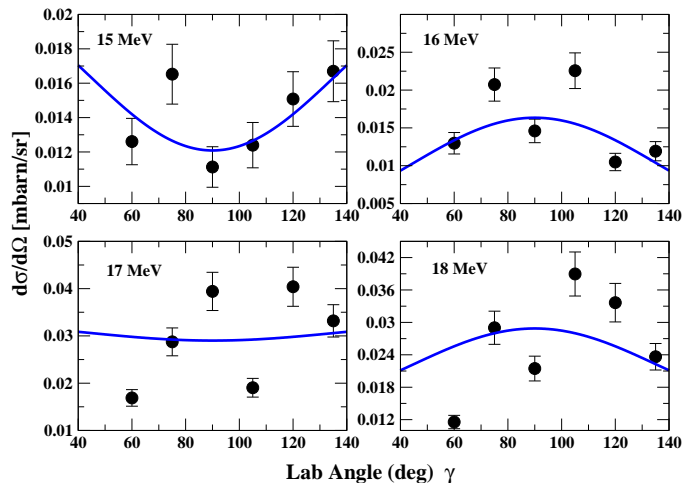


FIG. 10. Angular distribution of γ -rays obtained for 12.7 MeV state.

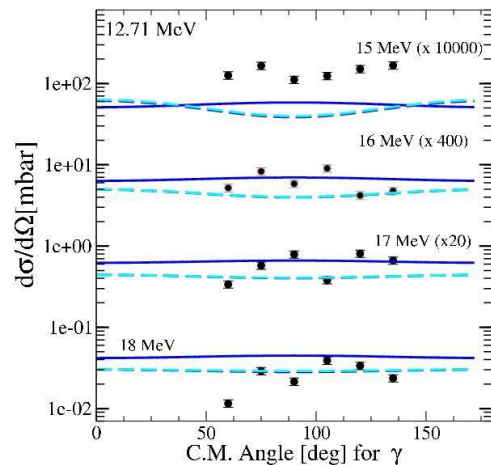


FIG. 11. The partial $(p, p'\gamma)$ differential cross-section for excitation to the 12.71 MeV (1^+) energy level. The gamma data are from this work. The blue lines are from the single particle model of this work. The solid line is the complete model without resonances added, the dashed line adds resonances listed in the Appendix A. The new light blue line has one additional resonance of the $l = 1$ state which are listed in the A.

transitions. The Fig. 3. shows a typical gamma-ray spectrum measured at 90° for a beam energy of 17 MeV. It is highly encouraging to see all the three gamma-rays namely, 9.64, 12.7 and 15.1 MeV with their well resolved first escape peaks. This is much higher quality data than reported earlier using a NaI(Tl) detector. The threshold values for the formation of 12.7 and 15.1 MeV states are 13.8 MeV, 16.8 MeV, respectively, for inelastic scattering of proton. The angular distribution of gamma-rays were carried out for four beam energies between 15 to 18 MeV and are shown in Fig. 10. The solid blue lines are fits to the data with Legendre polynomials. As mentioned in section 4.3, we extracted total cross sections from these fits.

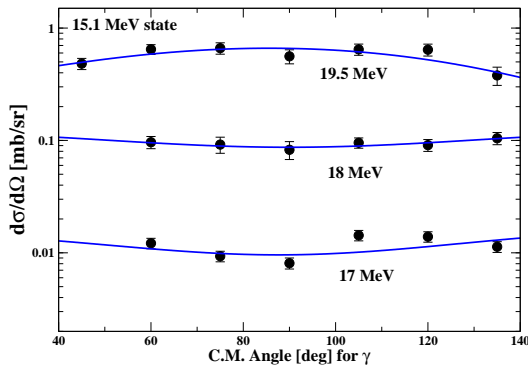


FIG. 12. Angular distribution of γ -rays obtained for 15.1 MeV state.

The same experimental data (gamma differential cross sections) are compared with theoretical calculations in Fig. 11. As in previous figures, the solid blue lines depict a calculation without resonances added. The dashed blue line includes the resonances given in Table-V. The light blue dashed line also includes two extra $l = 0$ resonances ((1) $E = 16.75 \text{ MeV}, \Gamma = 1.05 \text{ MeV}, \text{Strength} = 1.5E - 4$ $E = 21.75 \text{ MeV}, \Gamma = 1.95 \text{ MeV}, \text{Strength} = 2.5E - 4$). Similar to the 9.64 MeV state, the 12.71 MeV state is also predominantly an alpha emitter. The branching ratio to the ground state for gamma emission is 0.019 [10, 48]. We found the fraction to be close to 0.02 by comparing the total (p, p') cross-section and our measured $(p, p')\gamma$ cross-section for this state at 18 MeV beam energy. It can be seen from Fig. 11 that for 16, 17 and 18 MeV beam energies the data can be nearly reproduced by calculations with or without resonances. However, there is significant difference between theory and experiment for 15 MeV beam energy.

For the 15.1 MeV state the gamma differential cross sections were measured at three different beam energies, namely, 17, 18 and 19.5 MeV. The angular distributions are shown in Fig. 12 along with the Legendre polynomial fit (blue line). The same gamma differential cross sections are compared with theoretical calculations in Fig. 13. We observe in Fig. 13. that there is not significant difference between calculations with or without resonances. It has also to be noted that unlike the previous case of 12.71 MeV, there is significant difference in magnitudes of the experimental and theoretical cross sections. We also measured the 90° gamma differential cross sections for eight different beam energies. The data is shown in Fig. 15 and the inset shows the comparison of the same reported by Measday *et al.* [49]. This shows a very good match in overall shape between our measurements and those reported in Measday *et al.*, [49].

A good compilation of this important data set can be found in Ref. [10]. The dashed blue lines are the theoretical calculations carried out as a part of this work. The branching ratio to the ground state for gamma emission from the 15.1 MeV state is 0.087 [7]. We found the frac-

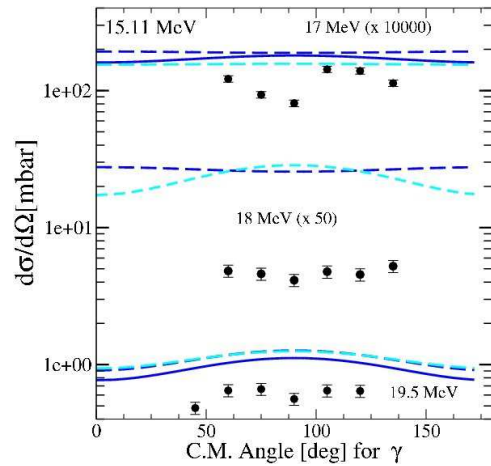


FIG. 13. The partial $(p, p'\gamma)$ differential cross-section for excitation to the 15.1 MeV (1^+) energy level. The gamma data are from this work. The blue lines are from the single particle model of this work. The solid line is the complete model without resonances added, the dashed line adds resonances listed in the Appendix A. The new light blue line has two additional resonances of the $l = 0$ and $l = 1$ state which are listed in the text.

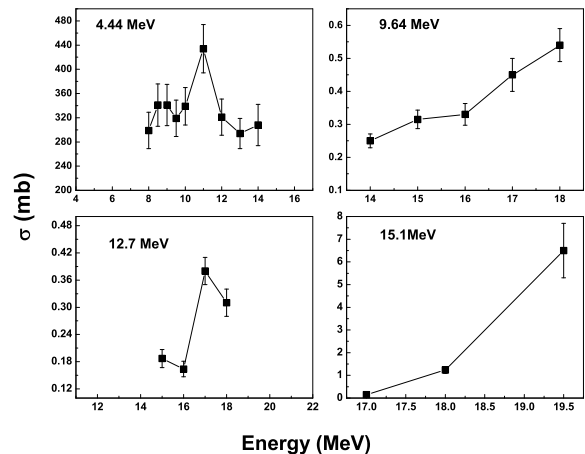


FIG. 14. Total measured cross section of ^{12}C states at 4.44 MeV, 9.64 MeV, 12.7 MeV and 15.1 MeV.

tion to be close to 0.079 which is given in Table -II. The gamma breaching ratios were calculated by taking the ratio of $\sigma_\gamma/\sigma_{pp'}$. The values of $\sigma_{pp'}$ cross sections were taken from Ref. [7, 19, 44] for 9.64, 12.71 and 15.1 MeV states. The results are shown in Table-II. We have chosen the beam energies to measure branching ratios in such a way that the desired states (namely, 9.64 MeV, 12.7 MeV and 15.1 MeV) should not be fed significantly from higher states. Therefore, the measured branching ratios will have lesser errors. Gamma branching ratios of 12.7 and 15.1 MeV states are in good agreement with the reported literature within the error bars. For the

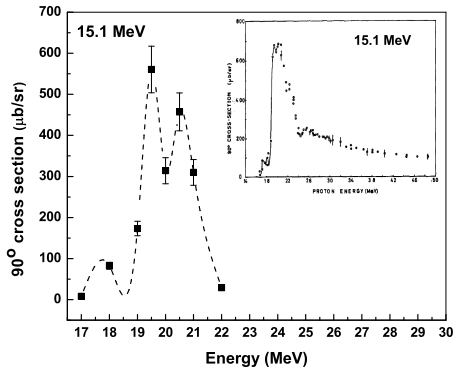


FIG. 15. A comparison 90° yield curve of present measurement of γ -rays obtained for the 15.1 MeV state at beam energies ranging from $E_p=17$ to 22 MeV, and inset showing the same data of Measday *et al.*,[49].

first time, we are reporting the gamma branching ratio of 9.64 MeV level. The total measured cross section data are shown in Fig. 14.

VI. SUMMARY

We have carried out exhaustive measurements of $(p, p' \gamma)$ cross sections for four excited states in ^{12}C , (4.44, 9.64, 12.7 and 15.1 MeV) for beam energies ranging from 8 to 22 MeV. These included angular distribution measurements for six different angles with respect to the beam direction. The full data set is summarised in Table-I. Gamma-ray spectra have been measured with a large volume $\text{LaBr}_3:\text{Ce}$ detector. In doing so, we have been able to record spectra with quality better than those obtained in the past by using $\text{NaI}(\text{Tl})$ detectors. We have extracted differential and total gamma cross sections for all four states at all beam energies. Our experimental data have been compared with rigorous theoretical optical model calculations. Overall, we have been successful in reproducing the experimental data except for the 15.1 MeV state where we found considerable mismatch between theory and experiment. From our theoretical analysis of the data we understand it is absolutely necessary to include various resonant states in the calculations. This has been seen while reproducing the differential gamma and total gamma cross sections for all four

states. We conclude that the 4.44 MeV is a collective state which agrees with the conclusion of previous studies. For the 9.64 MeV state, to the best of our knowledge, we have measured the cross sections and angular distributions of $(p, p' \gamma)$ for the first time. We have also extracted the gamma branching ratio of the 9.64 MeV state to the ground state for the first time. We conclude that the 9.64 MeV state is also a collective state. The conclusions are different for the possible structures of the 12.7 and 15.1 MeV states. These two states are possibly single-particle excitations. We have been unable to reproduce the data for 15.1 MeV state as well as for the three other states. The 15.1 MeV state is especially difficult because of its unnatural $T = 1$ and $M1$ transition character.

ACKNOWLEDGMENT

One of the authors (I.M) acknowledges the financial support from DST, Government of India, One of the authors (M.D) acknowledges the financial support from the Ministry of Human Resource Development, Government of India, and the author (G. Anil Kumar) acknowledges the partial financial support received from DST, Government of India as part of the fast track project (No: SR/FTP/PS-032/2011).

Appendix A: Appendixes

The solid blue line is the single particle model. At these energies it also is deficient. However the model has flexibility and methods have been developed to add resonance structure to it as described above. The resonance structure is included with the blue-dashed line. These resonances are all the isoscalar listed in the literature [37] but we made some choices made when unknown. Specifically for the 18.35 MeV resonance their has been discrepancy on the parity, we chose a 2^- state (see Refs. [46, 50]). Likewise there has been debate on what the J value is for the broad resonance at 21.6 MeV, we chose $J^\pi = 2^+$ following Ref. [47]. Strengths of the resonance were fit to the 4.44 MeV level data but we also used Refs. [47, 50] as a guide, again with the overall goal to see if the resonance addition help improve the calculations. Overall the result is an improvement, the best fits include the resonance structure.

-
- [1] K. Amos, P. J. Dortmans, H. V. von Geramb, S. Karataglidis, and J. Raynall. *Nucleon-Nucleus Scattering: A Microscopic Nonrelativistic Approach*. Springer US, Boston, MA, 2002.
- [2] J. P. Jeukenne, A. Lejeune, and C. Mahaux, Many-body theory of nuclear matter. *Physics Reports*, **25**, 83, 1976.

- [3] F. A. Brieva and J. R. Rook, Nucleon-nucleus optical model potential. *Nuclear Physics A*, **291**, 299, 1977.
- [4] J. S. Petler, M. S. Islam, R. W. Finlay, and F. S. Dietrich, Microscopic optical model analysis of nucleon scattering from light nuclei. *Phys. Rev. C*, **32**, 673, 1985.

| Resonance Energy MeV | J^π (T) | Width (Γ) MeV | Strength |
|-------------------------|-------------|---------------------------|----------|
| 7.65 | 0+ | 1.0E-5 | 6.0E-4 |
| 9.64 | 3- | 3.4E-2 | 7.5E-4 |
| 10.80 | 1- | 0.315 | 1.7E-4 |
| 11.83 | 2- | 0.260 | 1.4E-4 |
| 12.71 | 1+ | 2.0E-5 | 1.5E-5 |
| 15.44 | 2+ | 1.50 | 1.25E-3 |
| 18.35 | 2- | 0.35 | 2.0E-5 |
| 21.59 | 2+ | 1.20 | 4.0E-5 |
| 9.85* | 2+ | 1.01 | 2.5E-4 |
| 9.04* | 0+ | 1.45 | 7.5E-4 |
| 10.53* | 0+ | 1.42 | 1.0E-4 |

TABLE III. The isoscalar resonances chosen for the light blue dashed lines for the 4.44 MeV state. The resonances were found to be the smallest values that produced a similar total cross-section for the 4.44 MeV state. The strengths are all real. The states with * are new additions, note we removed the 10.3 MeV 0+ state and replaced it with two states. All electric transitions have a phase of 0, all magnetic transitions have a phase of π .

| Resonance Energy MeV | J^π (T) | Width (Γ) MeV | Strength |
|-------------------------|-------------|---------------------------|----------|
| 4.44 | 2+ | 1e-06 | 3.0E-3 |
| 7.65 | 0+ | 1.0E-5 | 6.0E-4 |
| 10.80 | 1- | 0.315 | 1.7E-4 |
| 11.83 | 2- | 0.260 | 1.4E-4 |
| 12.71 | 1+ | 2.0E-5 | 1.5E-5 |
| 15.44 | 2+ | 1.50 | 1.25E-3 |
| 18.35 | 2- | 0.35 | 2.0E-5 |
| 21.59 | 2+ | 1.20 | 4.0E-5 |
| 9.85 | 2+ | 1.01 | 2.5E-4 |
| 9.04 | 0+ | 1.45 | 7.5E-4 |
| 10.53 | 0+ | 1.42 | 1.0E-4 |
| 14.25* | 3- | 1.1 | 3.0E-4 |
| 18.6* | 3- | 0.35 | 3.8E-4 |
| 21.59* | 3- | 1.2 | 1.05E-3 |

TABLE IV. The isoscalar resonances chosen for the dark and light blue dashed lines of the 9.64 MeV state. The resonances were found to be the smallest values that produced a similar total cross-section for the 4.44 MeV state. The strengths are all real. The states with * are new additions for the light blue line for the 9.64 MeV state. All electric transitions have a phase of 0, all magnetic transitions have a phase of π . These resonances are nearly the same as for the 4.44 MeV state.

- [5] S. Kato, K. Okada, M. Kondo, K. Hosono, T. Saito, N. Matsuoka, K. Hatanaka, T. Noro, S. Nagamachi, H. Shimizu, K. Ogino, Y. Kadota, S. Matsuki, and M. Wakai, Inelastic scattering of 65 MeV protons from ^{12}C , ^{24}Mg , ^{28}Si , and ^{32}S . Phys. Rev. C, **31**, 1616, 1985.
- [6] S. P. Weppner. 'optical model analysis', *to be published*.
- [7] E. K. Warburton and H. O. Funsten, High-energy gamma rays and low-energy protons and deuterons from $\text{c}^{12} + p$ for $E_p = 14 - 20$ MeV. Phys. Rev., **128**, 1810, 1962.
- [8] D. F. Measday, M. Hasinoff, and D. L. Johnson, High-energy levels in ^{13}N . Canadian Journal of Physics, **51**(11), 1227, 1973.
- [9] D. Berghofer, M. D. Hasinoff, R. Helmer, S. T. Lim, D. F. Measday, and K. Ebisawa, High-energy levels in ^{13}N (II). Nuclear Physics A, **263**, 109, 1976.
- [10] A. Marcinkowski and B. Marianski, Compilation and evaluation of high energy gamma-ray standards from nuclear reactions. International Atomic Energy Agency, Vienna, Austria, Feb 1999. and references within.
- [11] P. Dyer, D. Bodansky, A. G. Seamster, E. B. Norman, and D. R. Maxson, Cross sections relevant to gamma-ray astronomy: Proton induced reactions. Phys. Rev. C, **23**, 1865, 1981.
- [12] F. L. Lang, C. W. Werntz, C. J. Crannell, J. I. Trombka, and C. C. Chang, Cross sections for production of the 15.10-MeV and other astrophysically significant gamma-ray lines through excitation and spallation of C-12 and O-16 with protons. Phys. Rev., **C35**, 1214, 1987.
- [13] K. T. Lesko, E. B. Norman, R.-M. Larimer, S. Kuhn, D. M. Meekhof, S. G. Crane, and H. G. Bussell, Measure-

| Resonance Energy MeV | J^π (T) | Width (Γ) MeV | Strength |
|-------------------------|-------------|---------------------------|----------|
| 4.44 | 2+ | 1e-06 | 3.0E-3 |
| 7.65 | 0+ | 1.0E-5 | 6.0E-4 |
| 9.64 | 3- | 0.034 | 7.5E-4 |
| 10.80 | 1- | 0.315 | 1.7E-4 |
| 11.83 | 2- | 0.260 | 1.4E-4 |
| 15.44 | 2+ | 1.50 | 1.25E-3 |
| 18.35 | 2- | 0.35 | 2.0E-5 |
| 21.59 | 2+ | 1.20 | 4.0E-5 |
| 9.85 | 2+ | 1.01 | 2.5E-4 |
| 9.04 | 0+ | 1.45 | 7.5E-4 |
| 10.53 | 0+ | 1.42 | 1.0E-4 |
| 14.25 | 3- | 1.1 | 3.0E-4 |
| 18.6 | 3- | 0.35 | 3.8E-4 |
| 21.59 | 3- | 1.2 | 1.05E-3 |
| 18.16* | 1+ | 0.24 | 3.0E-4 |

TABLE V. The isoscalar resonances chosen for the dark and light blue dashed lines for the 12.71 MeV state. The resonances were found to be the smallest values that produced a similar total cross-section for the 4.44 MeV state. The strengths are all real. The states with * are new additions for the light blue line for the 12.71 MeV state. All electric transitions have a phase of π , all magnetic transitions have a phase of 0 (since 12.71 MeV is a magnetic transition). These resonances are nearly the same as for the 4.44 MeV and 9.64 MeV states.

| Resonance Energy MeV | J^π (T) | Width (Γ) MeV | Strength |
|-------------------------|-------------|---------------------------|----------|
| 16.11 | 2+ | 5.0E-3 | 1.0E-4 |
| 16.57 | 2- | 0.3 | 3.0E-4 |
| 17.23 | 1- | 1.15 | 7.0E-4 |
| 17.76 | 0+ | 0.08 | 6e-05 |
| 18.35 | 3- | 0.22 | 9e-05 |
| 18.8 | 2+ | 0.1 | 8e-05 |
| 22 | 1- | 0.8 | 1.2E-4 |
| 22.65 | 1- | 3.2 | 1.5E-4 |
| 23.53* | 1- | 0.238 | 3.0E-4 |
| 23.99* | 1- | 0.57 | 5.0E-4 |
| 25.4* | 1- | 2.0 | 1.1E-3 |
| 23.75* | 0- | 3.0 | 1.5E-3 |

TABLE VI. The isovector resonances chosen for the dark and light blue dashed lines of the isovector 15.11 MeV state. These resonances do not have the same confidence level as the isoscalar transitions, they were fit only to the 15.11 MeV state. The strengths are all real. The states with * are new additions for the light blue line for the 15.11 MeV state. All electric transitions have a phase of π , all magnetic transitions have a phase of 0 (since 15.11 MeV is a magnetic transition).

- ments of cross sections relevant to γ -ray line astronomy. Phys. Rev. C, **37**, 1808, 1988.
- [14] J. Kiener, M. Berheide, N. L. Achouri, A. Boughrara, A. Coc, A. Lefebvre, F. de Oliveira Santos, and Ch. Vieu, γ -ray production by inelastic proton scattering on ^{16}O and ^{12}C . Phys. Rev. C, **58**, 2174, 1998.
- [15] J. Kiener, N. de Séréville, and V. Tatischeff, Shape of the 4.438 MeV γ -ray line of ^{12}C from proton and α -particle induced reactions on ^{12}C and ^{16}O . Phys. Rev. C, **64**, 025803, 2001.
- [16] J. Kiener. www.arxiv.org/abs/1710.03535v1/.
- [17] K. Gul, K. Shahzad, J. Taj, A. Awais, J. Hussain, F.J. Qureshi, and N. Ali, Experimental study of proton scattering on carbon. Nuclear Instruments and Methods in Physics Research Section B: Beam Interactions with Materials and Atoms, **269**, 2032, 2011.
- [18] F. C. Barker, G. D. Symons, N. W. Tanner, and P. B. Treacy, Levels of N13 near 7 MeV excitation (I). Nuclear Physics, **45**, 449, 1963.
- [19] W. W. Daehnick and R. Sherr, Energy dependence of elastic and inelastic scattering from c^{12} for protons between 14 and 19 MeV. Phys. Rev., **133**, 1964.

- [20] J. B. Swint, A. C. L. Barnard, T. B. Clegg, and J. L. Weil, Cross sections as a function of energy for the scattering of protons from ^{12}C . *Nuclear Physics*, **86**, 119, 1966.
- [21] Homer E. Conzett, Inelastic scattering of 12-MeV protons on lithium, carbon, magnesium, and silicon. *Phys. Rev.*, **105**, 1324, 1957.
- [22] H. Guratzsch, G. Hofmann, H. Mller, and G. Stiller, A study of proton scattering on ^{12}C and ^{13}C at 7 MeV. *Nuclear Physics A*, **129**, 405, 1969.
- [23] Shinsaku Kobayashi, Shoshichi Motonaga, Yoshiaki Chiba, Kenji Katori, Andreas Stricker, Takashi Fujisawa, and Takeshi Wada, Spin flip in the inelastic scattering of protons from ^{12}C at energies around 13.1 MeV resonance. *Journal of the Physical Society of Japan*, **29**, 1, 1970.
- [24] R. Ramaty, B. Kozlovsky, and R. E. Lingenfelter, Nuclear gamma-rays from energetic particle interactions. *The Astrophysical Journal Supplement Series*, **40**, 487, 1979.
- [25] E. L. Chupp, H. Debrunner, E. Flueckiger, D. J. Forrest, F. Golliez, G. Kanbach, W. T. Vestrand, J. Cooper, and G. Share, Solar neutron emissivity during the large flare on 1982 June 3. *The Astrophysical Journal*, **318**, 913, July 1987.
- [26] R. J. Murphy, B. Kozlovsky, and R. Ramaty, Gamma-ray spectroscopic tests for the anisotropy of accelerated particles in solar flares. *The Astrophysical Journal*, **331**, 1029, 1988.
- [27] R. J. Murphy, B. Kozlovsky, J. Kiener, and G. H. Share, Nuclear gamma-ray de-excitation lines and continuum from accelerated-particle interactions in solar flares. *The Astrophysical Journal Supplement Series*, **183**, 142, 2009.
- [28] pelletron webpage, <http://www.tifr.res.in/~pell/pelletron/index.php>
- [29] I. Mazumdar, D. A. Gothe, G. Anil Kumar, N. Yadav, P. B. Chavan, and S. M. Patel, Studying the properties and response of a large volume (946cm^3) $\text{LaBr}_3:\text{Ce}$ detector with γ -rays up to 22.5 MeV. *Nucl. Instrum. Methods A*, **705**, 85, 2013.
- [30] Srim web page, <http://www.srim.org/>.
- [31] I. Mazumdar, P. Sugathan, J. J. Das, D. O. Kataria, N. Madhavan, and A. K. Sinha, A large high-energy gamma-ray spectrometer at NSC. *Nucl. Instrum. Methods A*, **417**, 297, 1998.
- [32] Geant4 webpage, <https://geant4.web.cern.ch/geant4/>.
- [33] Stephane Chauvie, S Guatelli, V Ivanchenko, F Longo, A Mantero, B Mascialino, P Nieminen, Luciano Pandola, S Parlati, Luis Peralta, M.G. Pia, Michela Piergentili, P Rodrigues, S Saliceti, and A Tndade, Geant4 low energy electromagnetic physics. *IEEE Nuclear Science Symposium Conference Record*, **3**, 1881, 2004.
- [34] S. Hauf, M. Kuster, M. Bati, Z. W. Bell, D. H. H. Hoffmann, P. M. Lang, S. Neff, M. G. Pia, G. Weidenspointner, and A. Zoglauer, Validation of geant4-based radioactive decay simulation. *IEEE Transactions on Nuclear Science*, **60**(4), 2984, 2013.
- [35] nndc webpage, <https://www.nndc.bnl.gov/>.
- [36] A. C. L. Barnard, J. B. Swint, and T. B. Clegg, Cross sections as a function of angle and complex phase shifts for the scattering of protons from ^{12}C . *Nuclear Physics*, **86**(1), 130, 1966.
- [37] F. Ajzenberg-Selove, Energy levels of light nuclei $A = 11-12$. *Nuclear Physics A*, **506**(1), 1, 1990.
- [38] M. Itoh, H. Akimune, M. Fujiwara, U. Garg, H. Hashimoto, T. Kawabata, K. Kawase, S. Kishi, T. Murakami, K. Nakanishi, Y. Nakatsugawa, B.K. Nayak, S. Okumura, H. Sakaguchi, H. Takeda, S. Terashima, M. Uchida, Y. Yasuda, M. Yosoi, and J. Zenihiro, Study of the cluster state at $E_x=10.3$ mev in ^{12}C . *Nuclear Physics A*, **738**, 268, 2004.
- [39] M. Itoh, H. Akimune, M. Fujiwara, U. Garg, N. Hashimoto, T. Kawabata, K. Kawase, S. Kishi, T. Murakami, K. Nakanishi, Y. Nakatsugawa, B. K. Nayak, S. Okumura, H. Sakaguchi, H. Takeda, S. Terashima, M. Uchida, Y. Yasuda, M. Yosoi, and J. Zenihiro, Candidate for the 2^+ excited hoyle state at $E_x \sim 10$ mev in ^{12}C . *Phys. Rev. C*, **84**, 054308, 2011.
- [40] Y. Funaki, Hoyle band and α condensation in ^{12}C . *Phys. Rev. C*, **92**, 021302, 2015.
- [41] Evgeny Epelbaum, Hermann Krebs, Timo A. Lähde, Dean Lee, and Ulf-G. Meißner, Structure and rotations of the hoyle state. *Phys. Rev. Lett.*, **109**, 252501, 2012.
- [42] W. R. Zimmerman, M. W. Ahmed, B. Bromberger, S. C. Stave, A. Breskin, and Dangendorf *et al*, Unambiguous identification of the second $2+$ state in C^{12} and the structure of the hoyle state. *Physical review letters*, **110**(15), 152502, 2013.
- [43] Robert W. Peelle, Differential cross sections for the scattering of medium energy protons on carbon. *Phys. Rev.*, **105**, 1311, 1957.
- [44] Masahide HARADA, Yukinobu WATANABE, Akihisa YAMAMOTO, and Satoshi YOSHIOKA *et al.*, The $^{12}\text{C}(p, p'3\alpha)$ breakup reaction induced by 14, 18 and 26 mev protons. *Journal of Nuclear Science and Technology*, **36**, 313, 1999.
- [45] Takashi Fujisawa, Norio Kishida, Toshiyuki Kubo, Takeshi Wada, and Yoshiyuki Toba *et al.*, Analyzing power-polarization inequality in the inelastic scattering of protons on ^{12}C for incident energies from 22.0 to 29.0 MeV. *Journal of the Physical Society of Japan*, **50**(10), 3198, 1981.
- [46] G. H. Neuschaefer, M. N. Stephens, S. L. Tabor, and K. W. Kemper, Single proton stripping reactions to ^{12}C . *Phys. Rev. C*, **28**, 1594, 1983.
- [47] Bency John, Y. Tokimoto, Y.-W. Lui, H. L. Clark, X. Chen, and D. H. Youngblood, Isoscalar electric multipole strength in ^{12}C . *Phys. Rev. C*, **68**, 014305, 2003.
- [48] O. S. Kirsebom, M. Alcorta, M. J. G. Borge, M. Cubero, C. A. Diget, R. Dominguez-Reyes, and L. Fraile *et al.*, Observation of gamma delayed 3 alpha breakup of the 15.11 and 12.71 MeV states in ^{12}C . *Physics Letters B*, **680**(1), 44, 2009.
- [49] D. F. Measday, P. S. Fisher, A. Kalmykov, F. A. Nikolaev, and A. B. Clegg, The $^{12}\text{C}(p, p')^{12}\text{C}$ (12.71 and 15.11 MeV) reaction from threshold to 50 MeV. *Nuclear Physics*, **45**, 98, 1963.
- [50] A Kiss, C Mayer-Boricke, M Rogge, P Turek, and S Wiktor, Inelastic scattering of 172.5 mev particles by ^{12}C . *Journal of Physics G: Nuclear Physics*, **13**(8), 1067, 1987.